Direct energy transfer from photocarriers to Mn-ion system in II-VI diluted-magnetic-semiconductor quantum wells

M. K. Kneip, D. R. Yakovlev,* and M. Bayer
Experimentelle Physik II, University of Dortmund, D-44227 Dortmund, Germany

A. A. Maksimov and I. I. Tartakovskii
Institute of Solid State Physics, Russian Academy of Sciences, 142432 Chernogolovka, Russia

D. Keller, W. Ossau, and L. W. Molenkamp
Physikalisches Institut der Universität Würzburg, Am Hubland, D-97074 Würzburg, Germany

A. Waag
Institute of Semiconductor Technology, Braunschweig Technical University, D-38106 Braunschweig, Germany

The dynamical response of magnetic ion system to pulsed laser excitation is studied in $(Zn,Mn)Se/(Zn,Be)Se$ and $(Cd,Mn)Te/(Cd,Mg)Te$ quantum well structures. Contributions of a direct heating of the Mn system by photocarriers and an indirect heating via nonequilibrium phonons are distinguished. Their relative efficiency is measured at different excitation densities and over a wide range of Mn concentrations from 0.4 to 11%. For all studied regimes the direct energy transfer from carriers dominates in $(Zn,Mn)Se$ structures. In $(Cd,Mn)Te$ structures a regime where the direct heating is still prominent but weaker than the phonon contribution is found.

I. INTRODUCTION

Diluted magnetic semiconductors (DMS) based on II-VI materials with Mn ions are widely used nowadays as model objects for testing concepts for spintronics applications. In these materials Mn^{2+} magnetic ions substitute isoelectronically metal ions in the cation sublattice, which allows growing ternary alloys with a wide range of Mn concentrations up to 100%. These materials such as $(Zn,Mn)Se$ and $(Cd,Mn)Te$ have good structural quality and show strong band edge photoluminescence, which allows one to apply the broad spectrum of optical experimental techniques, in particular in magnetic field, for their studies.[1,2] By contrast, luminescence is poor in III-V DMS materials, such as $(Ga,Mn)As$.

Giant magneto-optical and magnetotransport effects known for DMS materials are due to the strong exchange interaction between the spins of free carriers and the localized magnetic moments of Mn ions. These effects are based on polarization of the carrier spins interacting with the magnetic ions, which in turn are polarized by an external magnetic field. As a result the magnitudes of the spectroscopic responses are proportional to the magnetization of the Mn spin system. Besides the strength of external magnetic field, the magnetization is determined by the temperature of the Mn spin system, which can differ from the bath temperature (i.e., lattice temperature). Therefore, a heating of the Mn system can strongly influence magneto-optical and magnetotransport properties.

In spintronic devices interaction with free carriers with excess kinetic energy (photogenerated or electrically injected) can cause heating of the Mn spin system. Fast exchange scattering of the carriers on the magnetic ions provides efficient energy transfer into the Mn system, but Mn cooling down to the bath temperature is slowed down by relatively long spin-lattice relaxation (SLR) times characteristic for low Mn concentrations of few percents.[3–5] Mn heating under laser excitation has been reported in Refs. 6–9 and studied in more detail in Refs. 5 and 10–22. Heating by an electrical current was observed for $(Cd,Mn)Te/(Cd,Mg)Te$ quantum wells (QWs)[23] and for $(Hg,Mn)Te/(Hg,Cd)Te$ QWs.[24] It has been shown, that depending on excitation conditions, the Mn temperature can be increased from a few up to a hundred Kelvins above the bath temperature.

There are two ways for transferring energy from hot carriers to the Mn spin system. A *direct* way is via carrier exchange scattering on the localized Mn spins. It is characterized by very short transfer times τ_{e-Mn} in the picosecond range. The exchange scattering provides simultaneous energy and spin transfer and, therefore, is sensitive to the carrier spin polarization.[6,16] Also excitation of the internal Mn^{2+} ion transition $^6A_1 \rightarrow {}^4T_1$ by energy transfer from excitonic states may contribute to this direct way.[25–27] An *indirect* transfer is mediated by phonons emitted by the free carriers. This mechanism is controlled by spin-lattice relaxation of Mn ions, which couples phonons with the Mn spin system. The relative contributions of direct and indirect transfers are still under debate. On one hand it has been shown that in $(Zn,Mn)Se$ QWs,[5,17] in n-type doped $(Cd,Mn)Te$ QWs,[16] and in undoped $(Cd,Mn)Te$ QWs under high excitation density[14,15] the direct transfer is dominant. On the other hand, the indirect transfer has been suggested as the leading mechanism in bulk $(Cd,Mn)Te$,[13] in $(Cd,Mn)Te$ QWs,[20] and in $(Cd,Mn)Se$ quantum dots.[21,22] It is clear now that the relative contribution can be related to the DMS material, to the

TABLE I. Technological parameters and experimental values for the studied $Zn_{1-x}Mn_xSe/Zn_{1-y}Be_ySe$ QW heterostructures.

Sample no.	Mn content, x	QW width [Å]	Be content, y	SLR time [μs]
#1 (cb1542)	0.004	100	0.06	960
#2 (cb1651)	0.012	150	0.06	600
#3 (cb2169)	0.035	100	0.06	11
#4 (cb886)	0.11	100	0.11	0.02–0.07

heterostructure design and to the excitation conditions, i.e., power and duration of laser pulses. However, a comprehensive picture of the energy transfer accounting for all these factors is far from being developed and additional experimental data is required here. An experimental difficulty in collecting established data is also caused by the problem of separating contributions from direct and indirect transfer when the laser pulse duration exceeds phonon lifetimes of about 1 μs.

In this paper we report on dynamical studies of the energy transfer from photocarriers to the Mn spin system by means of irradiation with intense laser pulses of short duration of about 10 ns. Time-resolved spectroscopy with resolution considerably shorter than the phonon lifetimes allows us to distinguish two ways of the energy transfer in time domain. The direct heating of the Mn system by carriers takes place only during the laser pulse action, but the indirect phonon heating lasts considerably longer. We examine diluted-magnetic-semiconductor quantum wells based on (Zn,Mn)Se and (Cd,Mn)Te with various Mn concentrations under different excitation conditions. In the discussion section we analyze typical examples of experimental regimes used by different groups to study Mn heating by means of photocarriers. The emphasis is placed on a possibility to distinguish direct and indirect ways of energy transfer from carriers to the Mn spin system.

II. EXPERIMENT

A. Samples

$Zn_{1-x}Mn_xSe/Zn_{1-y}Be_ySe$ heterostructures with quantum wells were grown by molecular beam epitaxy on (100)-oriented GaAs substrates. Mn content was varied from $x=0.004$ up to 0.11 and Be content in the barrier layers was $y=0.06$ or 0.11 to provide efficient confinement of both electrons and holes in the DMS quantum well layers. Structure parameters are given in Table I. The samples were nominally undoped, which means that the background electron density in the QWs does not exceed 10^{10} cm^{-2}. Further details of structure parameters and comprehensive information about their optical properties can be found in Refs. 17, 28, and 29. The $Cd_{0.985}Mn_{0.015}Te/Cd_{0.6}Mg_{0.4}Te$ sample (ct969) is a 75 Å/75 Å multiple QW structure with 50 periods. It was grown by molecular beam epitaxy on (100)-oriented CdTe substrate and is nominally undoped.

B. Experimental technique

Optical measurements were performed at a bath temperature $T=1.6$ K with samples immersed in pumped liquid he-

lium. Magnetic fields up to 7 T were applied parallel to the structure growth axis and to the direction of the collected light (Faraday geometry). The emission signal was analyzed for either right-hand σ^+ or left-hand σ^- circular polarization. A pulsed yttrium aluminum garnet (YAG) laser operating at wavelengths of 355 nm (third harmonic) and 532 nm (second harmonic) was used for optical heating of the Mn spin system. Pulse duration was about 7 ns, maximum peak intensity $\sim$1 kW, and repetition rate could be varied up to 10 kHz. Time resolved photoluminescence (PL) spectra with resolution of 2 ns were recorded by means of a gated charge-coupled-device (CCD) camera synchronized with the laser pulses.

Exciton recombination time in ZnSe and CdTe-based quantum wells is about 100 ps,[30,31] i.e., it is much shorter than the duration of the laser pulse. In order to get information about processes occuring on time scales longer than the laser pulse we provide additional illumination of the sample with a cw HeCd laser at 325 nm. Excitation density of this laser was kept below 0.1 W/cm^2, in order to minimize heating of the Mn system. Laser excitation spots were usually larger than $\sim$1 mm in diameter and only small central parts ($<$100 μm in diameter) of these spots were projected on an entrance slit of a 0.5 m monochromator. This allows us to avoid uncertainties caused by spatially inhomogeneous excitation. Further details of the experimental technique in application to (Zn,Mn)Se/(Zn,Be)Se heterostructures can be found in Ref. 28.

We are interested in the dynamical response of the magnetization on the laser impact. To measure that response, a finite equilibrium magnetization is induced by application of an external magnetic field. The magnetization evolution resulted from the impact pulses is detected by means of time-resolved photoluminescence. Excess kinetic energy of hot photocarriers, being transferred into the magnetic ion system, causes an increase of the Mn spin temperature T_{Mn}. We exploit the internal thermometer of T_{Mn}, which is provided by the high sensitivity of the giant Zeeman splitting of excitons (band states) to the polarization of the Mn spins. The latter can be conveniently received from the spectral position of the excitonic photoluminescence (PL) line measured in external magnetic fields.[14,17,28]

The giant Zeeman splitting ΔE_Z is proportional to the magnetization and thus to the average spin of the Mn ions $\langle S_z \rangle$,

$$\Delta E_Z = (\delta_e \alpha - \delta_h \beta) N_0 x \langle S_z \rangle. \quad (1)$$

Here $N_0\alpha = 0.26$ eV and $N_0\beta = -1.31$ eV are the exchange constants for the conduction and valence bands, respectively, in $Zn_{1-x}Mn_xSe$.[32] In $Cd_{1-x}Mn_xTe$ the constants are $N_0\alpha = 0.22$ eV and $N_0\beta = -0.88$ eV.[33] N_0 is the inverse unit-cell volume and x is the Mn mole fraction. The parameters δ_e and δ_h are introduced to account for the leakage of the electron and hole wave functions into the nonmagnetic barriers. In the studied structures they are very close to unity as carrier wave functions are localized in the DMS quantum wells. $\langle S_z \rangle$ represents the thermal average of the Mn spin along the magnetic field direction $B=B_z$ at a Mn spin temperature T_{Mn}. It can be expressed by the modified Brillouin function $B_{5/2}$,
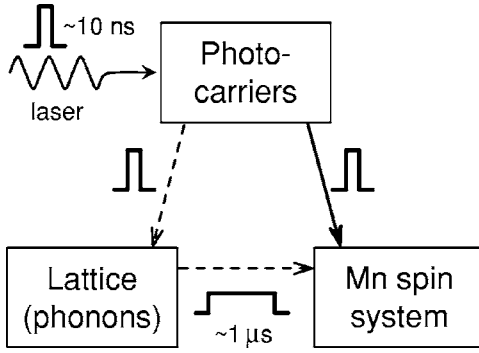
FIG. 1. Different paths of energy transfer from photocarriers excited by short laser pulses ($\sim$10 ns) to Mn spin system. The solid arrow shows the *direct* way taking place during the presence of photocarriers in the sample. The *indirect* way shown by dashed arrows involves nonequilibrium phonons generated by the free carriers during energy relaxation. The duration of this impact is given by typical lifetimes of nonequilibrium phonons of about 1 μs.

$$\langle S_z \rangle = -S_{eff}(x) B_{5/2} \left[\frac{5 g_{Mn} \mu_B B}{2 k_B [T_{Mn} + T_0(x)]} \right]. \qquad (2)$$

Here $g_{Mn} = 2$ is the g factor of Mn^{2+} ions, S_{eff} is the effective spin, and T_0 is the effective temperature. These parameters allow for a phenomenological account of the antiferromagnetic Mn-Mn exchange interaction (for their values see, e.g., Refs. 17 and 34).

In cases when the giant Zeeman splitting value ΔE_Z is measured from the energy shift of exciton transitions in reflectivity, absorption, or PL excitation spectra, Eqs. (1) and (2) allow direct access to T_{Mn} value. However, when it is measured from the shift of PL line a possible contribution of magnetic polaron formation should be taken into account.[35,36] For that, an external magnetic field B in Eq. (2) can be substituted by a sum of an external magnetic field and an exchange field in the magnetic polaron. We have checked experimentally that for the samples reported in this paper the magnetic polaron contribution to the giant Zeeman shift of PL line was very small. Therefore, we do not account for it in the data analysis.

III. EXPERIMENTAL RESULTS

Laser light being absorbed in a DMS structure generates photocarriers (electrons and holes) with excess kinetic energy. This energy can be transferred to the Mn spin system by two ways shown schematically in Fig. 1. The first way shown by the solid arrow is provided by exchange scattering of the free carriers on magnetic ions and leads to *direct* energy transfer. The second way (dashed arrows) is *indirect* and involves nonequilibrium phonons generated by the free carriers during the course of energy relaxation. Therefore, the laser pulses have double impact on heating the Mn system. These two impacts may differ in duration, time profile, and heating efficiency. Relative contributions of these impacts depend on the DMS material, the structure parameters, and the excitation conditions.[5,16,17,20,22] After the end of impact pulse the Mn system relaxes to the lattice temperature with a
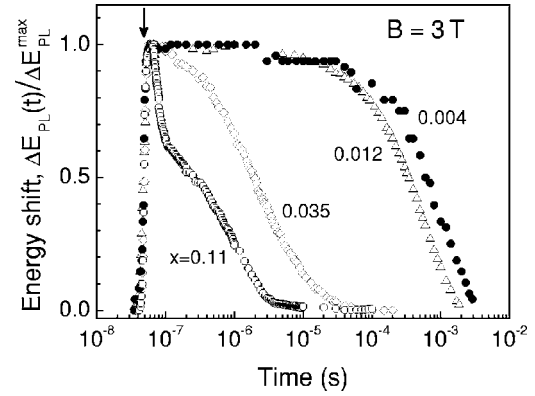

FIG. 2. Normalized energy shifts of PL lines induced by third harmonic (355 nm) YAG laser pulses at a magnetic field $B = 3$ T in different Zn$_{1-x}$Mn$_x$Se/Zn$_{1-y}$Be$_y$Se QWs (see Table I). The maximum shifts ΔE_{PL}^{max} are 5, 12, 23, and 26 meV for samples #1, #2, #3, and #4, respectively. The maximum of laser pulse is shown by the arrow. For convenient comparison of the different samples the data have been plotted on a logarithmic time scale. $T = 1.6$ K.

characteristic spin-lattice relaxation time. The spin-lattice relaxation in (Zn,Mn)Se structures has been studied by using pulsed photoexcitation in Ref. 28. In this paper we concentrate on the heating dynamics of the Mn spin system.

Characteristic parameters of the carrier and phonon impacts for the laser pulsed excitation can be found in Ref. 28. In short, they are as follows: Temporal profile of the laser pulse $I_L(t)$ has a Gauss shape with a full-width at a half maximum of $\sim$7 ns, as shown by the dashed line in Fig. 3. The carrier impact $I_c(t)$ almost coincides with the laser pulse $I_L(t)$, but the phonon impact $I_{ph}(t)$ differs from it. Nonequilibrium phonons are generated by the photocarriers dissipating their kinetic energy. Therefore, the leading edge of $I_{ph}(t)$ does not exceed $\sim$10 ns (i.e., integral of laser pulse), but the trailing edge is determined by the lifetime of acoustic phonons in crystals at low temperatures, which is on the order of 1 μs.[37] As a result, the Mn system is exposed to a short carrier impact and a long phonon impact, as is shown schematically in Fig. 1. The relative efficiency of these impacts for Mn heating can be characterized by the maximum temperature of the Mn system that resulted from them: Θ_c for the carrier impact and Θ_{ph} for the phonon impact.

Energy shifts of emission lines induced by third harmonic (355 nm) YAG laser pulses at a magnetic field $B = 3$ T are shown in Fig. 2 for Zn$_{1-x}$Mn$_x$Se/Zn$_{1-y}$Be$_y$Se QWs with Mn concentrations varied from 0.004 up to 0.11. For the sake of convenient comparison the data are normalized by the maximum shift achieved in each structure ΔE_{PL}^{max}. For the given experimental conditions ΔE_{PL}^{max} varies from 5 meV for $x = 0.004$ up to 26 meV for $x = 0.11$ and the Mn spin temperature was up to 15 K higher than the bath $T = 1.6$ K. Logarithmic scale for the time delay was chosen to highlight the huge dynamic range of SLR times from 20 ns up to 1 ms covered by the energy shift which reflects the cooling of the Mn spin system.[28] It is, however, remarkable that the heating of the Mn spin system (the rise of the signal) is very fast and identical for all samples.

The rising part is given in more detail in Fig. 3. The solid curve gives the integral of the laser pulse and corresponds
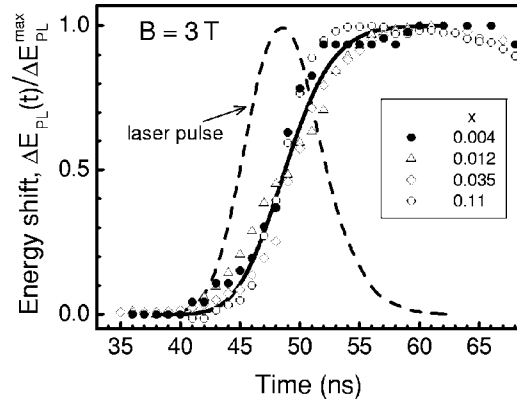
FIG. 3. Closeup of the initial parts of dynamic data in Fig. 2 to illustrate only the rise in energy in (Zn,Mn)Se based QWs with different Mn concentrations (the symbols) in comparison with the laser pulse integral (solid line). The dashed line shows the excitation laser pulse profile. The time scale is linear. $T=1.6$ K.

therefore to the expected carrier impact on direct Mn heating. One can see that experimental data for all concentrations are grouped closely around this curve. This allows us to conclude that in (Zn,Mn)Se QWs the direct energy transfer dominates over the indirect one. This is in good agreement with the results obtained earlier for cw laser excitation.[17]

We can use the spectral selectivity of the optical spectroscopy techniques to highlight the dynamical response of the Mn system to the phonon impact only. For that 532 nm wavelength laser pulses with a photon energy smaller than the band gap of (Zn,Mn)Se and (Zn,Be)Se were used. These photons are absorbed in the GaAs buffer layer, and the Mn system in (Zn,Mn)Se is exposed to the phonon flux from the GaAs, see Fig. 4(a). It should be noted that the delay of phonon impact on the magnetic ions in this case is negligible (less than 1 ns). That is due to the small distance (<1 μm) which nonequilibrium phonons generated in the GaAs buffer have to propagate to reach the (Zn,Mn)Se QW. In the sample with high Mn content $x=0.11$, where the SLR time τ_{SLR} $=20-70$ ns is considerably shorter than the phonon lifetimes of about 1 μs, the rise of the Mn response for 532 nm excitation is controlled by τ_{SLR} and its decay traces the phonon dynamics during their cooling to the bath temperature. It is shown by the closed circles in Fig. 4(b). Comparing this dependence with the data measured under 355 nm laser pulse illumination (the open circles) we can separate in time domain the contributions of the direct and indirect energy transfer mechanisms. For the given conditions the direct transfer induces $\Delta E_{PL}^{max} \approx 26$ meV, which corresponds to $\Theta_c \approx 17$ K, and the phonon contribution does not exceed 14 meV with $\Theta_{ph} \approx 6$ K.

In the $Zn_{0.985}Mn_{0.035}Se$ sample the SLR time τ_{SLR} $=11$ μs exceeds considerably the phonon lifetimes, in contrast to the case of the $Zn_{0.89}Mn_{0.11}Se$ QW in Fig. 4(b). As a result the rise of the Mn response under 532 nm excitation corresponds to the integral over the phonon pulse of about 3 μs (compare Figs. 4(c) and 4(b), the closed circles data). The decay of the Mn response follows the SLR with τ_{SLR} $=11$ μs and is identical for 532 nm and 355 nm excitation.

As we noted in the introduction, varying excitation conditions might change considerably the relative efficiency of
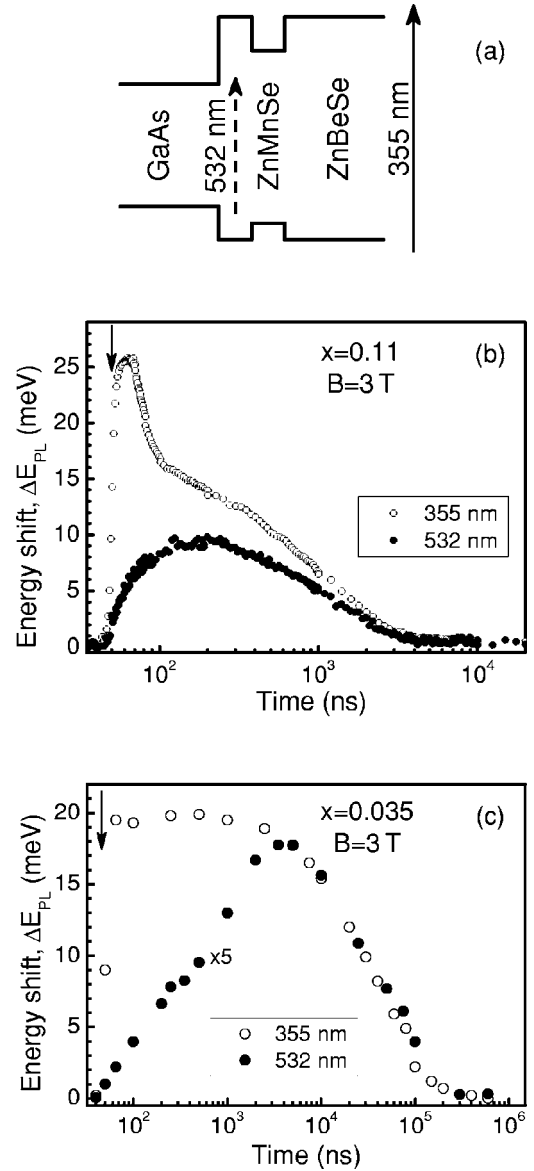

FIG. 4. (a) Energy scheme for the photoexcitation with different photons. 355 nm photons with energy of 3.49 eV generate carriers in (Zn,Mn)Se and (Zn,Be)Se, but 532 nm excitation with photon energy of 2.33 eV is absorbed only in GaAs buffer layer. In the latter case only *indirect* Mn heating by phonons is expected. (b) The temporal behavior of the PL peak energy shift ΔE_{PL} in $Zn_{0.89}Mn_{0.11}Se$ QW for two different excitation energies. The excitation density was 54 kW/cm^2 at 355 nm (open circles) and 30 kW/cm^2 at 532 nm (closed circles). (c) The temporal behavior of the PL peak energy shift ΔE_{PL} in a $Zn_{0.965}Mn_{0.035}Se$ QW under excitation with 355 nm (open circles) and 532 nm (closed circles) laser pulses with excitation density ~ 50 kW/cm^2. The vertical arrows in (b) and (c) show the laser pulse maximum position. T $=1.6$ K.

the direct and indirect energy transfer from photocarriers to the Mn spin system. For deeper insight for our experimental conditions, we performed measurements on the $Zn_{0.89}Mn_{0.11}Se$ QW for excitation densities varied from 0.5 up to 54 kW/cm^2. The results for the energy shift $\Delta E_{PL}(t)$ were converted into values of T_{Mn} and are collected in Fig. 5.
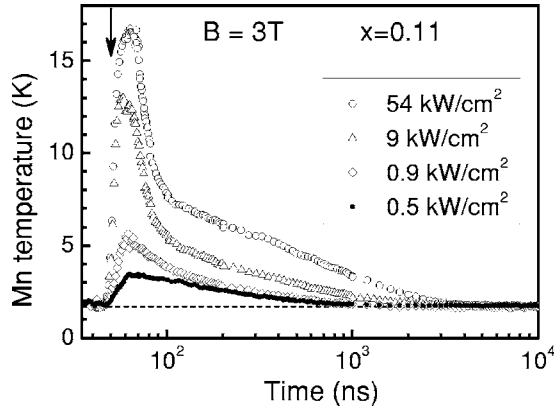
FIG. 5. Energy shift of the PL line converted into Mn spin temperature T_{Mn} versus time, measured at different excitation densities of 355 nm laser pulses for $Zn_{0.89}Mn_{0.11}Se/Zn_{0.89}Be_{0.11}Se$ QW. The vertical arrow indicates the laser pulse maximum. $T = 1.6$ K.

A pronounced peak at short delays caused by the direct transfer loses its dominance upon decreasing excitation density.

To quantify this behavior we plot in Fig. 6 the maximal T_{Mn} achieved by the direct and indirect transfers as function of excitation density. Θ_c was measured at a delay of 10 ns, i.e., just after the laser pulse, and Θ_{ph} was taken at delays of about 200 ns, which exceeds $\tau_{SLR} = 20-70$ ns for this sample.[28] It is seen that the carrier impact to the Mn heating increases rapidly with the excitation power increase. As for the phonon impact Θ_{ph}, its behavior can be fitted by the well-known dependence of the phonon system temperature T_{ph} under pulsed laser excitation $P \propto (T_{ph}^4 - T^4)$.[37] This result is a consequence of the phonon contribution to the specific heat which is proportional to T^3 at low temperatures. It should be noted that in the $Zn_{0.89}Mn_{0.11}Se$ sample $\Theta_c \geqslant \Theta_{ph}$ for the whole range of excitation densities studied.

In (Cd,Mn)Te QWs the situation can differ qualitatively from that in (Zn,Mn)Se QWs. As one can see in Fig. 7, in the $Cd_{0.985}Mn_{0.015}Te/Cd_{0.6}Mg_{0.4}Te$ sample the indirect heating is
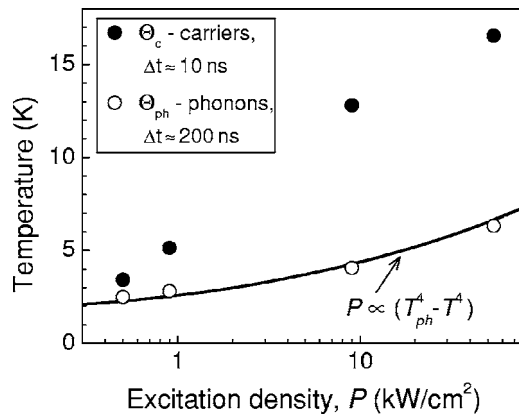

FIG. 6. Maximal Mn spin temperatures achieved by direct carrier heating Θ_c measured at $\Delta t \approx 10$ ns (closed circles) and by non-equilibrium phonons ($\Theta_{ph} = T_{ph}$), measured at $\Delta t \approx 200$ ns (open circles) as function of excitation density in $Zn_{0.89}Mn_{0.11}Se/Zn_{0.89}Be_{0.11}Se$ QW. The solid line describes a $P \propto (T_{ph}^4 - T^4)$ dependence (see text). $B = 3$ T, $T = 1.6$ K.

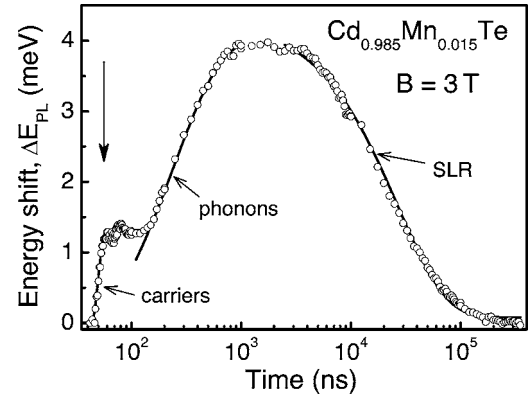FIG. 7. Temporal behavior of the PL line energy shift ΔE_{PL} in $Cd_{0.985}Mn_{0.015}Te/Cd_{0.6}Mg_{0.4}Te$ multiple QW. The *indirect* (phonon) heating is stronger in this sample than the *direct* heating through carriers. The dynamics of Mn heating allows for distinguishing contributions from carriers and nonequilibrium phonons. The solid lines represent at early times the integral of laser pulse (carriers), then the exponential growth with time constant ~ 0.3 μs due to phonons, and finally the monoexponential decay with a spin lattice relaxation (SLR) time of 28 μs. The vertical arrow shows the laser pulse maximum position. $T = 1.6$ K.

more efficient than the direct one: $\Theta_{ph} \approx 4.8$ K and $\Theta_c \approx 2.8$ K. Here $\tau_{SLR} = 28$ μs exceeds the phonon lifetimes and is therefore associated with the decay of the signal. Rise of the signal has two distinct parts. The fast but smaller in amplitude one is due to the direct energy transfer from photocarriers and the slow one is contributed by the indirect transfer involving nonequilibrium phonons. Figure 7 demonstrates clearly that the chosen experimental conditions, namely the short excitation pulses and the nanosecond time resolution, allow for isolating the direct carrier contribution even for the cases when $\Theta_c < \Theta_{ph}$.

IV. DISCUSSION

In most experimental situations the distinction between direct and indirect mechanisms of Mn heating by hot photocarriers is not a trivial task. It requires extended sets of experimental data (i.e., for different Mn concentrations, excitation densities, temperatures, and magnetic fields) and careful interpretation. Here we would like to discuss three typical examples of experimental situations.

Steady-state optical excitation does not give a direct access to the characteristic times and the magnitude of the heating effect, i.e., the Mn spin temperature is the main parameter for consideration. Very different T_{Mn} have been found in (Zn,Mn)Se QWs under the same excitation conditions.[17] At excitation density of about 10 W/cm² a sample with $x = 0.06$ shows $T_{Mn} = 3$ K, which gives a conservative estimate for the highest temperature of the phonon system. For the same conditions in an $x = 0.004$ sample $T_{Mn} = 42$ K due to direct heating of the Mn system by hot photocarriers has been found. For n-type doped (Cd,Mn)Te QWs efficient direct energy transfer has been concluded from the characteristic dependence of T_{Mn} on external magnetic field, which is not expected for the phonon contribution.[16] However, for un-

doped (Cd,Mn)Te QWs with x varied from 0.01 to 0.07 the importance of the indirect energy transfer via the phonons has been worked out.[20]

Long pulses with low and moderate excitation densities (typically $1-100$ W/cm^2). Usually external modulation of cw lasers is used for such experiments, which allows for easy adaptation of the pulse length for strongly varying SLR times in structures with different Mn concentrations. In such experiments performed for bulk (Cd,Mn)Te (Refs. 13 and 38) and (Cd,Mn)Se quantum dots,[21,22] the heating times after switching on the laser pulse were shorter but on the order of cooling times of the Mn system after the end of the pulse. It was also shown that the heating time depends on the excitation density and shortens by an order of magnitude with its increase.[38] The heating times were associated with the SLR times and on this basis the conclusion of a dominating role of indirect energy transfer involving phonons has been drawn. However, this conclusion might not always be valid. We would like to show below that a long heating time alone, even when it becomes comparable with SLR times, is not sufficient to conclude the dominant role of the indirect energy transfer.

To illustrate this, we have analyzed this situation on the basis of the approach developed in Ref. 16 and have written the following simplified energy balance equations for interacting systems of carriers and magnetic ions:

$$\frac{dE_{Mn}}{dt} = C_{Mn}\left(-\frac{\Delta T_{Mn}}{\tau_{SLR}} - \frac{\Delta T_{Mn}}{\tau_{Mn-e}} + \frac{\Delta T_e}{\tau_{Mn-e}}\right), \qquad (3)$$

$$\frac{dE_e}{dt} = C_e\left(-\frac{\Delta T_e}{\tau_{e-L}} - \frac{\Delta T_e}{\tau_{e-Mn}} + \frac{\Delta T_{Mn}}{\tau_{e-Mn}}\right) + G_e. \qquad (4)$$

Here, ΔT_{Mn}, ΔT_e are the deviations of the Mn ions and carriers temperatures from the lattice temperature; C_{Mn} and C_e are their specific heats; $\tau_{e-Mn} = \tau_{Mn-e}C_e/C_{Mn}$, τ_{SLR}, and τ_{e-L} are the characteristic times for equalizing the temperatures of carriers and magnetic ions, magnetic ions and lattice, and carriers and lattice, respectively. G_e is the energy flux from external sources into the carrier subsystem (e.g., due to generation of hot photocarriers). For the sake of simplicity we do not take into account heating of the lattice itself under low and moderate photoexcitation densities. It should be noted that typical values of τ_{e-Mn} and τ_{e-L} are on the order of $1-100$ ps, and $\tau_{SLR} > 10$ ns for the typical DMS samples under consideration, i.e., it is always valid that τ_{e-Mn}, τ_{e-L} $\ll \tau_{SLR}$. The ratio between τ_{e-Mn} and τ_{e-L} determines the relative contribution of the *direct* and *indirect* paths for Mn heating which we have discussed above. The other small parameter in our equations, which is the ratio $C_e/C_{Mn} \ll 1$, is due to the fact that for typical experimental conditions the concentration of photoexcited carriers is always much smaller than the concentration of Mn ions in DMS samples with $x \geq 0.001$.

With these assumptions it can be easily shown that the characteristic time for heating of the Mn system after switching on the photogeneration (which corresponds to the rise time of the signal in experiment) is described by

$$\tau_{in} = \left(\frac{1}{\tau_{SLR}} + \frac{C_e}{C_{Mn}} \cdot \frac{1}{\tau_{e-Mn} + \tau_{e-L}}\right)^{-1} = \left(\frac{1}{\tau_{SLR}} + \frac{1}{\tau^*}\right)^{-1}. \qquad (5)$$

One can see from Eq. (5) that the rise time τ_{in} is controlled by the shorter of the two times τ_{SLR} and τ^*. There are several important consequences that can be drawn from this simplified model:

(i) First, the rise time τ_{in} should be always much longer than the τ_{e-Mn} and τ_{e-L} times, giving the energy flux rates from carriers to the Mn spin system and to the phonon system (lattice), respectively. Indeed, if $\tau_{SLR} \ll \tau^*$, then $\tau_{in} \approx \tau_{SLR}$. On the other hand for $\tau_{SLR} \gg \tau^*$, the following relation holds: $\tau_{in} \approx \tau^* = (\tau_{e-Mn} + \tau_{e-L})C_{Mn}/C_e$, and the factor $C_{Mn}/C_e \gg 1$ becomes important.

(ii) To have $\tau_{in} \approx \tau_{SLR}$ the second term in Eq. (5) should be much smaller than the first one, i.e., $\tau_{SLR} \ll \tau^*$. It is remarkable, that this criterion provides no restriction for the relative ratio of the τ_{e-Mn} and τ_{e-L} times. Therefore, $\tau_{in} \approx \tau_{SLR}$ can occur even in a situation with dominating *direct* energy transfer (see Fig. 1) when the energy flux from carriers to the Mn system is much faster than to the lattice $\tau_{e-Mn} \ll \tau_{e-L}$. This means that the experimental observation of Mn heating with the spin relaxation time is not sufficient to conclude a dominant role of the *indirect* heating process.[13,22,38]

Short-pulse high-density excitation realized by means of pulsed lasers. Experiments for generating a dense electron-hole plasma in (Cd,Mn)Te/(Cd,Mg)Te QWs have been reported in Refs. 14, 15, and 39. When heating very fast during 0.5 ns, high peak temperatures of the Mn spin system and formation of spatial domains with elevated Mn temperatures are arguments for a dominating contribution of the direct energy transfer in these experiments. The moderate excitation density regime, but with high time resolution down to 2 ns, is reported in the present paper. As we have shown, direct and indirect contributions can be distinguished in time domain. The direct transfer dominates in (Zn,Mn)Se structures for all studied Mn contents from 0.004 to 0.11. The indirect energy transfer is more efficient in Cd$_{0.985}$Mn$_{0.015}$Te QWs.

V. CONCLUSIONS

In this paper we have experimentally addressed the problem of energy transfer from hot carriers to the Mn spin system of DMS heterostructures. The hot photocarriers were generated by laser pulses, whose duration of about 10 ns is considerably shorter than the typical lifetime of nonequilibrium acoustical phonons of about 1 μs. Following the evolution of the Mn spin temperature in time domain, we were able to distinguish clearly the contribution of the direct energy transfer from the indirect one mediated by the phonon system. It has been shown that over a wide range of Mn concentrations and excitation densities the direct energy transfer dominates in (Zn,Mn)Se heterostructures.

The physical reasons for the different dominances of direct and indirect paths of energy transfer in (Zn,Mn)Se and (Cd,Mn)Te require further clarification. Detailed study of

(Cd,Mn)Te with different Mn concentrations is needed, which is beyond the scope of the present paper. Exchange scattering times of carriers on magnetic ions should not differ strongly in these materials as the exchange constants $N_0\alpha$ and $N_0\beta$ do not differ considerably [see values given after Eq. (1)]. We can suppose that the stronger indirect path in (Cd,Mn)Te is related to stronger nonradiative recombination known for this material in comparison with (Zn,Mn)Se. As a result a larger part of photocarrier energy is converted to the phonon system and then reaches the Mn spin system via the indirect path.

For the sake of simplicity we discuss in this paper only the energy transfer from hot free carriers to the Mn system. This is correct for the indirect transfer involving nonequilibrium phonons. The direct transfer via carrier-Mn spin exchange scattering is based on the flip-flop process and therefore combines energy *and* spin transfer (see, e.g., Refs. 11 and 16). Further experiments with spin oriented photocarriers generated by circular polarized light in the vicinity of the band gap are planned to address this problem.

*Also in A. F. Ioffe Physico-Technical Institute, Russian Academy of Sciences, 194021 St. Petersburg, Russia.

[1] J. K. Furdyna, J. Appl. Phys. **64**, R29 (1988).

[2] T. Dietl, *Handbook of Semiconductors*, edited by S. Mahajan (North-Holland, Amsterdam, 1994), Vol. 3b, p. 1252.

[3] D. Scalbert, Phys. Status Solidi B **193**, 189 (1996).

[4] A. V. Scherbakov, A. V. Akimov, D. R. Yakovlev, W. Ossau, G. Landwehr, T. Wojtowicz, G. Karczewski, and J. Kossut, Phys. Rev. B **62**, R10641 (2000).

[5] D. R. Yakovlev, M. Kneip, A. A. Maksimov, I. I. Tartakovskii, M. Bayer, D. Keller, W. Ossau, L. W. Molenkamp, A. V. Scherbakov, A. V. Akimov, and A. Waag, Phys. Status Solidi C **1**, 989 (2004).

[6] S. M. Ryabchenko, Yu. G. Semenov, and O. V. Terletskii, Sov. Phys. JETP **55**, 557 (1982) [Zh. Eksp. Teor. Fiz. **82**, 951 (1982)].

[7] J. Frey, R. Frey, and C. Flytzanis, Phys. Rev. B **45**, 4056 (1992).

[8] D. Wolverson, S. V. Railson, M. P. Halsall, J. J. Davies, D. E. Ashenford, and B. Lunn, Semicond. Sci. Technol. **10**, 1475 (1995).

[9] V. F. Aguekian, D. E. Ashenford, B. Lunn, A. V. Koudinov, Yu. G. Kusraev, and B. P. Zakharchenya, Phys. Status Solidi B **195**, 647 (1996).

[10] H. Krenn, W. Zawadzki, and G. Bauer, Phys. Rev. Lett. **55**, 1510 (1985).

[11] H. Krenn, K. Kaltenegger, T. Dietl, J. Spalek, and G. Bauer, Phys. Rev. B **39**, 10918 (1989).

[12] J. J. Baumberg, S. A. Crooker, D. D. Awschalom, N. Samarth, H. Luo, and J. K. Furdyna, Phys. Rev. B **50**, 7689 (1994).

[13] W. Farah, D. Scalbert, and M. Nawrocki, Phys. Rev. B **53**, R10461 (1996).

[14] V. D. Kulakovskii, M. G. Tyazhlov, A. I. Filin, D. R. Yakovlev, A. Waag, and G. Landwehr, Phys. Rev. B **54**, R8333 (1996).

[15] M. G. Tyazhlov, A. I. Filin, A. V. Larionov, V. D. Kulakovskii, D. R. Yakovlev, A. Waag, and G. Landwehr, Sov. Phys. JETP **85**, 784 (1997) [Zh. Eksp. Teor. Fiz. **112**, 1440 (1997)].

[16] B. König, I. A. Merkulov, D. R. Yakovlev, W. Ossau, S. M. Ryabchenko, M. Kutrowski, T. Wojtowicz, G. Karczewski, and J. Kossut, Phys. Rev. B **61**, 16870 (2000).

[17] D. Keller, D. R. Yakovlev, B. König, W. Ossau, Th. Gruber, A. Waag, L. W. Molenkamp, and A. V. Scherbakov, Phys. Rev. B **65**, 035313 (2002).

[18] D. Keller, D. R. Yakovlev, Th. Gruber, A. Waag, W. Ossau, L. W. Molenkamp, F. Pulizzi, P. C. M. Christianen, and J. C. Maan, Phys. Status Solidi B **229**, 797 (2002).

[19] T. Kuroda, F. Minami, and S. Seto, Phys. Status Solidi B **229**, 757 (2002).

[20] A. V. Koudinov, Yu. G. Kusrayev, and I. G. Aksyanov, Phys. Rev. B **68**, 085315 (2003).

[21] A. Hundt, J. Puls, A. V. Akimov, and F. Henneberger, Phys. Status Solidi C **2**, 867 (2005).

[22] A. Hundt, J. Puls, A. V. Akimov, Y. H. Fan, and F. Henneberger, Phys. Rev. B **72**, 033304 (2005).

[23] B. König, Ph.D. thesis, University of Würzburg, Germany 2000.

[24] Y. S. Gui, C. R. Becker, J. Liu, M. Konig, V. Daumer, M. N. Kiselev, H. Buhmann, and L. W. Molenkamp, Phys. Rev. B **70**, 195328 (2004).

[25] D. Some and A. V. Nurmikko, Phys. Rev. B **48**, 4418 (1993).

[26] D. Leinen, Phys. Rev. B **55**, 6975 (1997).

[27] H. Falk, J. Hübner, P. J. Klar, and W. Heimbrodt, Phys. Rev. B **68**, 165203 (2003).

[28] M. K. Kneip, D. R. Yakovlev, M. Bayer, A. A. Maksimo v, I. I. Tartakovskii, D. Keller, W. Ossau, L. W. Molenkamp, and A. Waag, Phys. Rev. B **73**, 045305 (2006).

[29] B. König, U. Zehnder, D. R. Yakovlev, W. Ossau, T. Gerhard, M. Keim, A. Waag, and G. Landwehr, Phys. Rev. B **60**, 2653 (1999).

[30] D. R. Yakovlev, J. Puls, G. V. Mikhailov, G. V. Astakhov, V. P. Kochereshko, W. Ossau, J. Nürnberger, W. Faschinger, F. Henneberger, and G. Landwehr, Phys. Status Solidi A **178**, 501 (2000).

[31] V. Ciulin, P. Kossacki, S. Haacke, J.-D. Ganiere, B. Deveaud, A. Esser, M. Kutrowski, and T. Wojtowicz, Phys. Rev. B **62**, R16310 (2000).

[32] A. Twardowski, M. von Ortenberg, M. Demianiuk, and R. Pauthenet, Solid State Commun. **51**, 849 (1984).

[33] J. A. Gaj, R. Planel, and G. Fishman, Solid State Commun. **29**, 435 (1979).

[34] W. J. Ossau and B. Kuhn-Heinrich, Physica B **184**, 442 (1993).

[35] G. Mackh, W. Ossau, D. R. Yakovlev, A. Waag, G. Landwehr, R. Hellmann, and E. O. Göbel, Phys. Rev. B **49**, 10248 (1994).

[36] D. R. Yakovlev and K. V. Kavokin, Comments Condens. Matter Phys. **18**, 51 (1996).

[37] J. Shah, R. F. Leheny, and W. F. Brinkman, Phys. Rev. B **10**, 659 (1974); A. V. Scherbakov, A. V. Akimov, D. R. Yakovlev, W.

Ossau, A. Waag, G. Landwehr, T. Wojtowicz, G. Karczewski, and J. Kossut, Phys. Rev. B **60**, 5609 (1999).

[38] D. Scalbert, W. Farah, and M. Nawrocki, *Proceedings of the 23rd International Conference on Physics of Semiconductors, Berlin, Germany, 1996*, edited by M. Scheffler and R. Zimmermann (World Scientific, Singapore, 1996), p. 433.

[39] M. G. Tyazhlov, V. D. Kulakovskii, A. I. Filin, D. R. Yakovlev, A. Waag, and G. Landwehr, Phys. Rev. B **59**, 2050 (1999).